Multi-scale modeling of the urban meteorology: integration of a new canopy model in the WRF model

Dasaraden Mauree[a,b,*], Nadège Blond[a], Alain Clappier[a]

[a] *Université de Strasbourg, CNRS, Laboratoire Image Ville Environnement (LIVE), UMR7362, Strasbourg, France*

[b] *Solar Energy and Building Physics Laboratory, Ecole Polytechnique Fédérale de Lausanne, Lausanne, Switzerland*

Abstract

Urban parametrizations have been recently developed and integrated in mesoscale meteorological models for a better reproduction of urban heat islands and to compute building energy consumption. The objective of the present study is to evaluate the value of the use of a module able to produce highly resolved vertical profiles of these variables. For this purpose, the Canopy Interface Model (CIM) was integrated as an additional urban physics option in the Weather Research and Forecasting model. The coupling method is here detailed and its evaluation is done using a reference run based on a fine resolution WRF simulation. In order to keep both the CIM and the mesoscale model coherent, an additional term is added to the calculation of the CIM. Finally, the BUBBLE dataset is used to validate the simulation of the profiles from CIM. It is demonstrated that the proposed coupling improves the simulations of the variables in an urban grid and that the WRF+CIM+BEP-BEM system can provide highly resolved vertical profiles while at the same time improving significantly computational time. The data from these preliminary results are very promising as it provides the foundation for the CIM to act as an interface between mesoscale and microscale models.

Keywords: Atmospheric boundary layer, Multiscale meteorological modeling, Turbulence paramterization, Urban canopy parametrizations, Urban meteorology

1. Introduction

Meteorological mesoscale models were initially dedicated to weather forecasting without the need to detail interactions between urban areas and the atmosphere (Salamanca et al., 2011; Ching , 2013). In the last few years, urban parametrizations have been integrated in these mesoscale models to also simulate urban heat islands (UHI) (Masson, 2000; Kusaka et al., 2001; Martilli et al., 2002; Kanda et al., 2005; Liu et al., 2006; Kusaka and Kimura, 2004; Sarkar and De Ridder, 2011), building energy consumption (Krpo et al., 2010) and air pollution at the urban scale (Salamanca et al., 2011). Different schemes have been developed in recent years with the underlying purpose of developing systems that could help urban planners make decisions and propose sustainable urban planning scenarios to decrease UHI, building energy demand, or urban air pollution. Baklanov et al. (2009) gave a guideline for the level of complexity that is needed for urban canopy parametrizations based on the "fitness for purpose". For air quality, urban climatology, strategies to mitigate UHI and urban planning, it is necessary to have more detailed and precise meteorological vertical profiles and fluxes.

*Corresponding author

Email address: dasaraden.mauree@gmail.com (Dasaraden Mauree)

It is now well known that the urban climate depends on a series of processes taking place at different spatial (from global to local) and temporal scales (Oke, 1982), and that building energy demand and urban climate are closely related and interdependent (Ashie et al., 1999; Kikegawa et al., 2003; Salamanca et al., 2011). However using mesoscale meteorological models, with a high vertical resolution, to cover a whole urban area and resolving at the same time local building effects and UHI is still not feasible with actual computer performances (Martilli, 2007). Moreover the use of available microscale models (such as Envimet (Bruse and Fleer, 1998), CitySim (Robinson, 2012) or EnergyPlus (Crawley et al., 2008)) on more than a neighborhood (few streets) is also not feasible. Thus multi-scale modeling is often suggested and used as a solution.

Garuma (2017) has recently reviewed urban surface parameterizations. Models developed by Masson (2000) or Kusaka and Kimura (2004), have been integrated in mesoscale models. However since they are single-layered models they do not calculate high resolution vertical profiles in the urban canopy. Using the same method as Martilli et al. (2002); Kondo et al. (2005), who used a multi-layer model, Muller (2007) designed experiments to show that a canopy module can be used for an enhanced coupling with mesoscale models while at the same time reducing the computational cost. However in their work, the canopy model developed by Muller (2007) was not totally independent of the mesoscale model and hence cannot be easily introduced in another model. Furthermore, the canopy model resolves flow in the vertical direction and hence is neglecting the horizontal advection that is considered in a mesoscale model. Inconsistencies will thus arise between computations done with a multi-layer microscale model such as BEP-BEM and a mesoscale model. One way to ensure coherence in regional climate models, is to use nudging techniques to reduce errors between the driving field and the simulated field (Pohl and Crétat, 2014; Omrani et al., 2015).

The Canopy Interface Model (CIM) that was recently developed and tested in an offline mode (Mauree, 2014; Mauree et al., 2015, 2017a) is here introduced in the Weather Research and Forecasting (WRF) community research model v3.5 (Skamarock et al., 2005, 2008). The objective is to build a multi-scale urban meteorological system that is able to produce highly resolved vertical profiles of meteorological variables in low-resolution mesoscale meteorological models. Additionally, the CIM can resolve the flow in two directions in the urban canopy. These profiles could thus be used to improve the computation of surface fluxes of momentum, heat, turbulent kinetic energy and humidity inside the mesoscale model and to allow at the same time for the coupling of a mesoscale model with a microscale model. Such a coupling between the CIM and CitySim, a micro-scale model to evaluate energy fluxes at the neighbourhood scale, has recently been implemented (Mauree et al., 2017b,c; Mauree et al., 2018; Perera et al., 2018).

The objective of the present article is to detail the steps followed to set up and evaluate the coupling. In Sect. 2 a brief description of the governing equations in WRF is given. In Sect. 3 it will be explained how the CIM has been integrated into WRF in order to keep in coherence both the mesoscale model and the CIM In Sect. 4 a description of the experiments conducted with WRF is presented. In Sect. 5 the results from a series of sensitivity tests are presented to evaluate the value of the use of the CIM and the coupling. Finally, the coupled system is ran over the City of Basel and the results from the simulations are compared with observations made during the BUBBLE experiment perfomed in Basel (Rotach et al., 2005). The last section is devoted to the discussions and the conclusions of this study.

2. Weather Research and Forecasting model

The Advanced Research Weather Research Forceast (WRF) (Skamarock et al., 2005, 2008), version 3.5, developed by the National Center for Atmospheric Research (NCAR) for research

purpose, is used in the present study. A broad variety of physics and dynamics options have been defined by the scientific community. Only a brief description of the conservation equations and the physics options that are used to simulate the surface layer is given here. The objective of this section is mainly to help understand the coupling of the CIM with WRF, which will be fully described in Sect. 3.

2.1. Governing equations and turbulent closure

Following Ooyama (1990), variables with conservation properties (mass for example) are written with equations in their flux form and using a terrain-following mass vertical coordinate. We here present briefly these equations to prepare the presentation of the coupling with the CIM.

Momentum and Heat

The following equation represents the conservation of momentum or heat.

$$\partial_t N + (\nabla . \vec{F_N})_\eta = F_N^s, \tag{1}$$

where N is the momentum for the x-, y- or z-directions or the heat and F_N^s is the source or sink terms from the surface. The second term on the left hand side of the equation is a flux divergence term which represents the advection, the pressure-gradient and the diffusion terms. The latter is a function of the diffusion coefficients, $K_{h,v}$ which is described later. The $\nabla . \vec{F_N}$ term depends the eta (η) levels and the latter can be computed using:

$$\eta = \frac{(p_h - p_{ht})}{\alpha}, \tag{2}$$

where p_h is the hydrostatic pressure at this height and p_{ht} is the pressure at the top boundary. α is the mass per unit area within the column in the domain and is calculated as $\alpha = p_{hs} - p_{ht}$ where p_{hs} is the pressure at the surface.

1.5 order turbulence closure

WRF provides several closure formulations for the calculation of the turbulent diffusion coefficients. A 1.5 order turbulence closure, using the turbulent kinetic energy (denoted hereafter as e, $(m^2 s^{-2})$) is chosen here. With this closure the turbulent diffusion coefficient can be computed using:

$$K_{h,v} = C_k l_{h,v} \sqrt{E}, \tag{3}$$

where the subscript h, v represent horizontal and vertical directions respectively, C_k is a constant, $l_{h,v}$ is a parametrized mixing length, proportional to the height and E is αe.

Turbulent Kinetic Energy

The e can be calculated using the following prognostic equation:

$$\partial_t (E) + (\nabla . \vec{F_E})_\eta = \alpha (P + G - \varepsilon), \tag{4}$$

where P and G represent the mechanical and buoyancy turbulence production terms respectively and ε is the dissipation term.

More details on the chosen formulations can be found in Skamarock et al. (2008).

2.2. Focus on specific physics schemes

WRF provides a large variety of physics schemes to represent different processes taking place in the atmosphere. For the purpose of this study, the focus is mainly on specific schemes that relate to future uses of the CIM.

Surface layer scheme

The surface layer schemes, available in WRF, calculate the friction velocities and exchange coefficients that enable the computation of surface heat and moisture fluxes by the land-surface models and surface stress in the Planetary Boundary Layer (PBL). The Monin-Obukhov Similarity Theory (Monin and Obukhov, 1954) option was chosen for this study.

Land-Surface Model

The Land-Surface Model (LSM) is a 1-D column model computing surface fluxes over land and sea-ice grid point starting from land-surface properties and outputs of the surface layer scheme and the radiation scheme. These fluxes give a lower boundary condition for the vertical transport done in the PBL schemes. The Noah LSM (Chen and Dudhia, 2001) was selected.

Multiple urban physics options are available in WRF (UCM, BEP, BEP-BEM). We have chosen to use the BEP-BEM parameterization (Salamanca et al., 2010) to simulate the buildings effects on the long wave and short wave radiation (shadow effects and multi-reflexion) and the surface fluxes of momentum and heat.

The Building Effect Parametrization (BEP) module is based on the multi-layer model from Martilli et al. (2002). Obstacle effects are estimated in several layers of the WRF model. It takes into account the 3-D geometry of urban surfaces as well as the ability of buildings to diffuse sources and sinks of heat and momentum vertically through the whole urban canopy layer. The Building Energy Model (BEM), developed by Krpo et al. (2010), computes the building energy balance (and the associated building demand) to keep a comfortable temperature inside buildings. This energy balance takes into account the effect of anthropogenic heating and heat diffusion through surfaces, radiation exchange through windows. The surface fluxes are computed at each level of the urban grid and aggregated in BEP and are used as input in the surface layer scheme.

Planetary Boundary Layer

The PBL scheme calculates flux profiles so as to compute the temperature, moisture and vertical momentum profiles for the atmosphere. One important aspect of these types of schemes is that they are one dimensional and assume that there is a clear separation between resolved and subgrid eddies (Skamarock et al., 2008). For the purpose of this study, the Bougeault and Laccarère turbulence closure scheme (Bougeault and Lacarrère, 1989) will be used to compute $l_{h,v}$, needed for the calculation of the diffusion coefficient in the WRF model.

3. Canopy Interface Model integration in WRF

A 1-D Canopy Interface Model (CIM) was developed by Mauree et al. (2017a) in order to improve low-resolution mesoscale meteorological models or to be used as an interface between low-resolution meteorological mesoscale model and microscale models. After a brief description of the CIM, it is explained in the present section how the CIM was introduced in WRF. CIM is independent of the mesoscale meteorological model and can hence also be run in an offline model. CIM can be typically forced at the top of the column and the variables are then calculated at the centre of each cell along the vertical axis.

3.1. Canopy Interface Model

The CIM solves 1-D transport equations, i.e. only the terms in the z-direction are kept from Eq. 1.

$$\frac{\partial u}{\partial t} = \frac{\partial}{\partial z}\left(\mu_t \frac{\partial u}{\partial z}\right) + f_u^s \tag{5}$$

$$\frac{\partial \theta}{\partial t} = \frac{\partial}{\partial z}\left(\kappa_t \frac{\partial \theta}{\partial z}\right) + f_\theta^s, \tag{6}$$

where u is the mean wind speed in the x- or y- directions (ms^{-1}), θ is the mean potential temperature (K), f_u^s and f_θ^s are the momentum and heat surface fluxes and μ_t and κ_t are the turbulent diffusion coefficients. κ_t is μ_t divided by the Prandtl number (0.95).

The CIM solves these equations using a 1.5 order turbulence closure based on the e. The diffusion coeffcient can be calculated using:

$$\mu_t = C_k l \sqrt{e}, \tag{7}$$

where C_k is a coefficient calculated to be equal to $k^{\frac{4}{3}}$, from Mauree et al. (2017a), where k is the von Kàrmàn constant (0.41), l is the mixing length (m) and e is calculated independently as follows:

$$\frac{\partial e}{\partial t} = \frac{\partial}{\partial z}\left(\lambda_t \frac{\partial e}{\partial z}\right) + C_\varepsilon^* \frac{\sqrt{e}}{l}(e_\infty - e) + f_e^s, \tag{8}$$

where λ_t is here assumed to be equal to μ_t (Muller, 2007) and e_∞ is a stationary e value as explained by Mauree et al. (2017a) and can be expressed as:

$$e_\infty = \frac{C_k}{C_\varepsilon^*} l^2 \left(\frac{\partial U}{\partial z}\right)^2 (1 - C_G \cdot Ri_f), \tag{9}$$

where U is the horizontal wind speed (ms^{-1}), C_ε^* is equal to 1 and C_G is a correction coefficient for the buoyancy term.

Further details on the development of the CIM, its governing equations and the calculation of the fluxes used in the model can be found in Mauree et al. (2017a).

3.2. WRF-CIM coupling strategy

The CIM computes highly resolved vertical profiles of various meteorological variables, but it does not include horizontal fluxes computed in models such as WRF (see Eq. 1). In such a context, it is possible to force the CIM with WRF in a one-way nesting but it will not be valuable to correct the values calculated by WRF using the CIM values as it could have been in a traditional two-way nesting.

Thus two methodologies are tested : the first one is based on a coupling using fixed top boundary conditions as done by Muller (2007); the second is a new proposition to add an additional term in the CIM calculation in order to account for the processes described by the flux divergence term in Eq. 1.

Coupling by Fixing Top boundary condition (Method FT)

The CIM can calculate vertical profiles using prescribed top boundary conditions and the geometry and surface temperature of the surface obstacles at each level of the grid (see Fig. 1). In an offline mode, the boundary conditions may be fixed at the top with a constant value. When coupled with the WRF model, this value is linearly interpolated from the mesoscale model at each timestep (Martilli et al., 2002). At the initialization timestep, the mesoscale values are

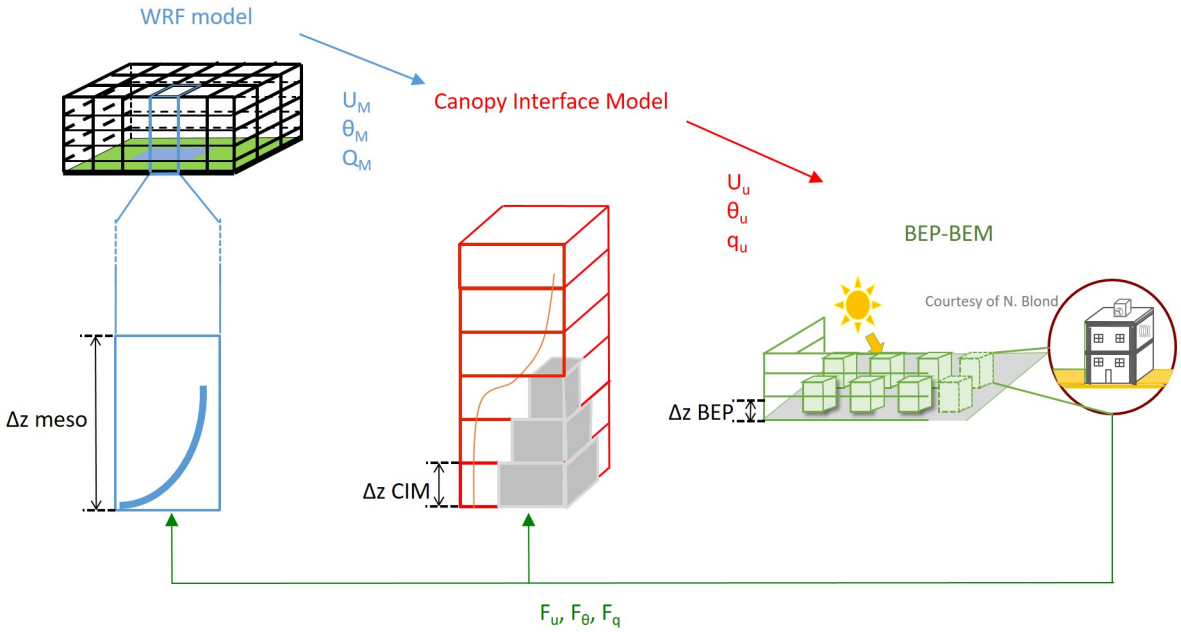

Figure 1: WRF scheme with the implementation of the CIM *(arrows and variables in blue denotes items from WRF, in red from the CIM and in green from BEP-BEM)*

interpolated on each of the CIM vertical level and used to initialize the computation of the surface fluxes done by the BEP-BEM system (Krpo et al., 2010). At other timesteps, the CIM high-resolution vertical profiles (wind speed, temperature and humidity) are given to BEP-BEM which proceeds to a potentially more detailed estimation of sources/sinks. The sources and sinks are fedback to the CIM to compute new vertical profiles, and to the mesoscale model (the surface fluxes are in this way aggregated at each of the mesoscale vertical levels and represent the F_N^s terms in the Eq. 1).

This coupling may be enough when the mixing boundary layer is well developed but could be limited in stable conditions when the exchanges between air layers are low. In such cases the horizontal fluxes cannot be neglected as compared to the vertical fluxes and this method will not conserve the coherence between the two models from a flux standpoint.

Coupling by Fixing Fluxes (Method FF)

To keep the coherence between the models, we propose in this section a method, similar to a nudging technique, to take into account the horizontal transport in the CIM as well as a new forcing term at the top of the CIM using fluxes. To develop this, an analysis of the budget of the fluxes is done over the vertical column of the CIM and for the corresponding volume from the mesoscale model. Figure 2 gives a representation of the fluxes considered in both the CIM and the WRF model. The following hypotheses can be made to ensure the coherence between the models and a balance of the fluxes:

- The mean value of each variable calculated on the CIM column should be the same as the one computed by the WRF mesoscale model (both models proposing an estimation of the same real profiles);

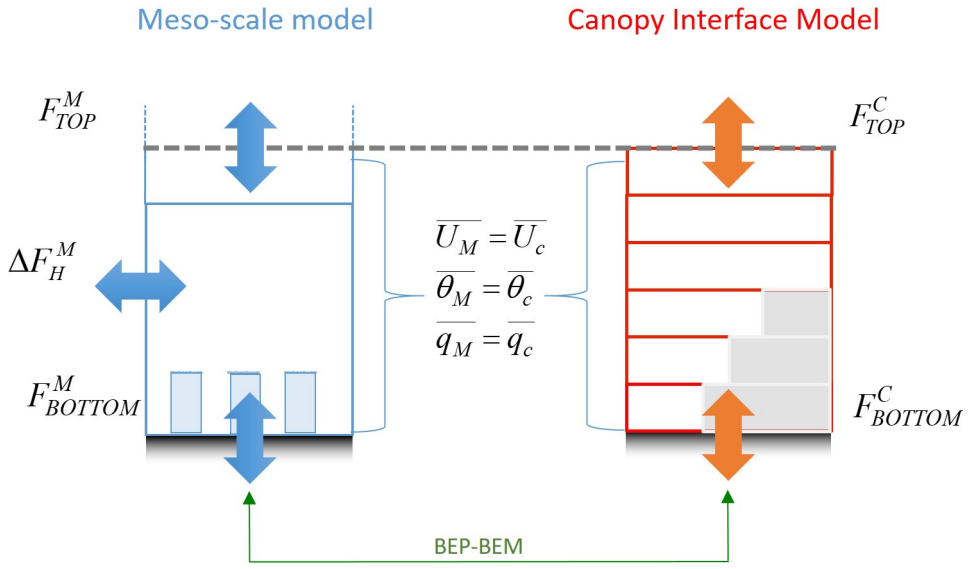

Figure 2: Representation of fluxes calculated on the vertical column in the CIM (right) before correction and in the corresponding volume in WRF (left). The average values from the WRF mesoscale model and from the CIM should be equal in both models for the same volume. The grey dashed line represent the top most level of the CIM and can be higher than the first level of the WRF mesoscale model.

- Bottom surface fluxes (i.e., all surface fluxes calculated to take into account the effects of obstacles at each level of the column) are computed once for forcing both the WRF mesoscale model and the CIM. The values should hence be equal in both models (F^M_{BOTTOM}=F^C_{BOTTOM}=F_{BOTTOM});
- In the WRF model, the fluxes are aggregated in BEP and used in the constant-flux theory (F^M_{BOTTOM}=F^M_{TOP});
- Far enough from the surface, the flux at the top of both columns should be equal as it would be less influenced by surface effects (F^M_{TOP}=F^C_{TOP}=F_{BOTTOM}).

Based on the above statements, the CIM profiles may be corrected after each timestep using an estimation of the horizontal fluxes. The formulation is done to allow computation of these values that are not known *a priori* in order to ensure a coherence between the models. Equation 10 points out the consequences of this condition on the CIM new profiles.

$$N_i^{Ct+1} = \begin{cases} N_i^{C*} + \Delta F_{Hi}, & \text{for } i < n \\ N_n^{C*} + \Delta F_{Hi} - \Delta t F_{TOP}, & \text{for } i = n, \end{cases} \tag{10}$$

where N is one of the variables calculated by the CIM (wind speed, potential temperature or humidity), t is the timestep considered, i is an index corresponding to the centre of a grid cell in the CIM and n is the number of levels in the urban grid. N_i^{Ct+1} is the updated vertical value of the CIM considering that N_i^{C*} is a first computation of the CIM without considering the horizontal fluxes and ΔF_{Hi} the horizontal terms to be added. A different equation is suggested for the top most level of the CIM with N_n^{C*} being the value computed by the CIM without considering the top flux, Δt is the time step and F_{TOP} the flux at the top as explained before

(and is oriented in the z-direction). This top flux may be used, instead of forcing the boundary conditions at the top of the CIM with values of wind, temperature or humidity.

To ensure coherence between the models using these formulations, we can write that the mean value of the variables calculated by the CIM have to be equal to the WRF mesoscale value:

$$\overline{N_i^{Mt+1}} = \overline{N_i^{Ct+1}} = \overline{N_i^{C*}} + \overline{\Delta F_{Hi}} - \frac{\Delta t F_{TOP}}{n}, \tag{11}$$

where $\overline{N_i^{Mt+1}}$ is the mean value interpolated from the WRF model over the n levels present in the CIM column similar to what is performed by Martilli et al. (2002). As a first approximation, the horizontal terms can be assumed constant over the CIM column (equal to their mean) and these are computed using Eq. 11 as:

$$\Delta F_{Hi} = \overline{\Delta F_{Hi}} = \overline{N_i^{Mt+1}} - \overline{N_i^{C*}} + \frac{\Delta t F_{TOP}}{n}. \tag{12}$$

This leads to Eq. 13, which gives the new formulations used in the CIM.

$$N_i^{Ct+1} = \begin{cases} N_i^{C*} + \overline{N_i^{Mt+1}} - \overline{N_i^{C*}} + \frac{\Delta t F_{TOP}}{n}, & \text{for } i < n \\ N_n^{C*} + \overline{N_i^{Mt+1}} - \overline{N_i^{C*}} + \frac{\Delta t F_{TOP}}{n} - \Delta t F_{TOP}, & \text{for } i = n \end{cases} \tag{13}$$

Based on this formulation, it can be expected that the the computation of the variables from the CIM and the WRF mesoscale model would be consistent and the departures between the driving and driven fields would be reduced.

4. Experiments with WRF-CIM

4.1. Evaluation of the coupling methods

A series of simulation are designed to assess the value of the use of the CIM in WRF and particularly to see how the CIM can improve the meteorological vertical profiles when using a coarse vertical resolution and its impact on the computational time.

A domain of 20*20 cells was designed and each cell has a horizontal resolution of 45 km*45 km. The domain was centered at latitude 48.404 °N and longitude 2.248 °E, situated near the "Ile-de-France" region in France, such that the topography did not interfere with the tests that have been conducted. The influence of the topography will be studied in future paper. A homogeneous urban area of 9 cells at the centre of the domain has been designed with building heights of 25m and the land use for the rest of the domain was taken from the MODIS database. In these simulations, the CIM consists of 15 vertical grid cell each 5m high to allow the constant-flux layer to develop above the building rooftop (Rotach, 1999). The aim of these simulations is to demonstrate the validity of the coupling methods. We have thus chosen this setting, run multiple simulations with various scenarios to determine which method would be more useful and to see the relevance of using only BEP-BEM as opposed to CIM-BEP-BEM.

Several simulations were performed with WRF, all using the urban parametrization BEP-BEM (see Table A.5), over a winter period of 30 days from the 27th of January 2010 at 0000 LT to the 26th of February 2010 at 0000 LT (with the first three days of initialization not being discussed here). We chose to focus on the winter period as the objective of the current development is to provide high-resolution profiles to microscale models that could be used to evaluate energy use in urban areas. We also ran experiments for the summer time but only briefly describe the results in this paper.

Table 1: Set of experiments run for theoretical case.

Simulations	Designation	Vertical resolution	Method
BEP-BEM	Ref.	Fine res. - 5m (15 levels)	
BEP-BEM	C1	Coarse res. - 94m (1 level)	
CIM+BEP-BEM	C3	Coarse res. - 94m (1 level)	FF
CIM+BEP-BEM	C5	Coarse res. - 94m (1 level)	FT

FF (fixed flux) and FT (fixed top) represent the two coupling methods.

WRF is run for all the simulations using the BEP-BEM parameterization for the urban effects. The vertical resolution, the use of CIM and the choice of the method are changed for the different scenarios:

Reference Simulation (Ref.) : WRF is run with a fine vertical resolution of 5 m (corresponding to the vertical resolution of the CIM) for the first 15 levels), without the CIM. This is considered to be the reference simulation. The simulation integrates all processes needed to calculate highly resolved vertical profiles used by BEP-BEM for computing the urban effects.

Simulation C1 : WRF is run with a coarse vertical resolution of 94 m, for the first level, without the CIM. This simulation, compared to the reference one, will show the impact of the vertical resolution on the surface representation and on the calculation of the meteorological variables in the WRF model.

Simulation C3 : WRF is run with a coarse vertical resolution with the CIM coupled using Method FF. BEP-BEM runs with the CIM profiles. This test is performed to see how the profiles that are calculated by the CIM, when it is integrated in the WRF model, correspond to those from the reference simulation and how this will in turn influence the mesoscale processes in a low resolution simulation.

Simulation C5 : WRF is run with a coarse vertical resolution with the CIM coupled using Method FT. This test is perfomed to compare with the FF method in a low resolution simulation.

It should be highlighted here that we consider the Ref. simulation as a controlled experiment which we can use to assess the coupling methods (FF and FT) and it can be relied on as the scheme that integrates most of the physical processes. Addtionally another set of simulation is performed to evaluate the impact of using a high resolution in WRF and this is included in Appendix A.

4.2. Validation of CIM integration in WRF

To validate the integration of CIM in WRF, a set of simulation was run over Basel for a period of 14 days from the 1 January 2002 at 0000 LTto the 15th of January 2002 at 0000 LT. Two scenarios were performed one with WRF+BEP-BEM and one with WRF+CIM+BEP-BEM. The four domains centred over the City of Basel with the different domains having a horizontal resolution of 45km, 15km, 3km and 1km respectively. The domain was designed using the WRFDomain wizard, allowing an optimal number of eta levels in the 1km and also for describing the bounding boxes. The GRIB data was downloaded from the UCAR dataset (NCEP et al., 2000). CSV files with the values (from CIM and as calculated by WRF) of the horizontal wind speed in both directions and the temperature for each vertical level were obtained from the simulation for comparison with measured data from the BUBBLE experiment (Rotach et al., 2005). All the data from BUBBLE and the simluation were averaged over one hour.

5. Results

This section aims at evaluating the coupling between the CIM and WRF and to justify the strategy that has been developed. As previously mentioned, the simulations presented here were performed for a period of 30 days (with the first three days of initialization not being discussed here) in January 2010. We only show results for the horizontal wind speed and the temperature for this corresponding period.

5.1. Global comparisons on specific vertical levels

We present here the comparisons over 27 days of simulation, in January, and a series of statistical tests in order to show the general trends when the CIM is integrated in WRF in winter. Table 2 summarizes the comparisons in terms of mean deviations (M.D.), correlations and the root mean square deviations (R.M.S.D.) computed on hourly values of the simulated temperatures and wind speeds. Figure 3 presents a time-evolution of the different simulations at 5 m and 50 m. The results from each scenario as compared to the reference case are discussed below.

5.1.1. Effect of the WRF vertical resolution - (Ref./C1)

We focus here on the differences observed between the fine and coarse resolution WRF simulations, without the CIM, as increasing the vertical resolution can have a significant impact on the temperature and the wind speed. It can be seen from Table 2 that, on average, the coarse WRF configuration (C1) generally tends to compute higher the potential temperatures and to simulate significantly lower the wind speed as compared to the reference simulation.

Figure 3a shows that the differences in temperature may be more than 2 K for some hours. The horizontal wind speed calculated at 50 m is weaker in the coarse resolution simulation than in the fine resolution simulation and these differences may reach 4 $\mathrm{m\,s^{-1}}$. These first results hence justify the development of the CIM model and its coupling with WRF since the changes in the vertical resolution have a notable impact on the accuracy of models to calculate temperature and wind profiles.

5.1.2. Effect of the FF coupling with the CIM at low resolution - (Ref./C3)

When using a coarse resolution in the model, the integration of the CIM in WRF drastically diminish the average deviations for the wind speed, from $-1.9\ \mathrm{m\,s^{-1}}$ to $-0.9\ \mathrm{m\,s^{-1}}$ at 50 m and reduces the difference in the temperature from 0.3 K to 0.1 K (see Table 2). It can however also be noted that in some cases the temperature is still lower by about 1 K. If we focus on the high vertical resolution profiles that the CIM produces, the discrepancy for wind speed as compared to the Ref. simulation is even decreased to $-0.6\ \mathrm{m\,s^{-1}}$ at 50 m while also respecting their variability (high correlation coefficient). Although the wind speed from the CIM at 50 m is generally in agreement with the Ref. simulation, there are a few hours where the difference can be up to 1 $\mathrm{m\,s^{-1}}$ (see Fig. 3b). However, the CIM computes a lower wind speed at 5 m (bias of $-1.2\ \mathrm{m\,s^{-1}}$) and the variability of these values is not as well represented, at the surface, as compared to the values obtained at 50 m. But as shown in Fig. 3d the amplitude is also less important at 5 m than at 50 m height. It is worthy to note that there are significant periods when the CIM has a very good correspondence with the fine resolution simulation.

Table 2: Statistical comparison between the Reference Simulation (Ref.) and simulations C1, C3 and C5.

Simulations	**Method**				
	FF	**FT**	**M.D.**	**R.M.S.D.**	**R**
For Potential Temperature (K)					
WRF+BEP-BEM					
Meso outputs at 50 m					
Coarse Res. C1			0.3	0.9	0.98
WRF+CIM+BEP-BEM					
Meso outputs at 50 m					
Coarse Res. C3	x		0.1	0.9	0.98
Coarse Res. C5		x	0.0	0.9	0.98
CIM outputs at 50 m					
Coarse Res. C3	x		0.0	1.0	0.98
Coarse Res. C5		x	0.1	0.9	0.98
CIM outputs at 5 m					
Coarse Res. C3	x		0.3	0.9	0.98
Coarse Res. C5		x	0.7	1.2	0.98
For Wind ($m\ s^{-1}$)					
WRF+BEP-BEM					
Meso outputs at 50 m					
Coarse Res. C1			-1.9	2.0	0.98
WRF+CIM+BEP-BEM					
Meso outputs at 50 m					
Coarse Res. C3	x		-0.9	1.0	0.98
Coarse Res. C5		x	-0.2	0.9	0.97
CIM outputs at 50 m					
Coarse Res. C3	x		-0.6	0.9	0.97
Coarse Res. C5		x	-0.2	0.7	0.98
CIM outputs at 5 m					
Coarse Res. C3	x		-1.2	1.5	0.59
Coarse Res. C5		x	-1.2	1.6	0.36

Comparisons are made for all the WRF outputs and for the CIM outputs for scenarios C3 and C5. FF (fixed flux) and FT (fixed top) represent the two coupling methods. M.D. represents the mean deviation from the reference simulation, R.M.S.D. is the root mean square deviation and R is the correlation. Meso outputs refers to outputs from the WRF mesoscale model, CIM outputs refers to outputs directly from CIM and 5m and 50m refers to the height at which the data is taken.

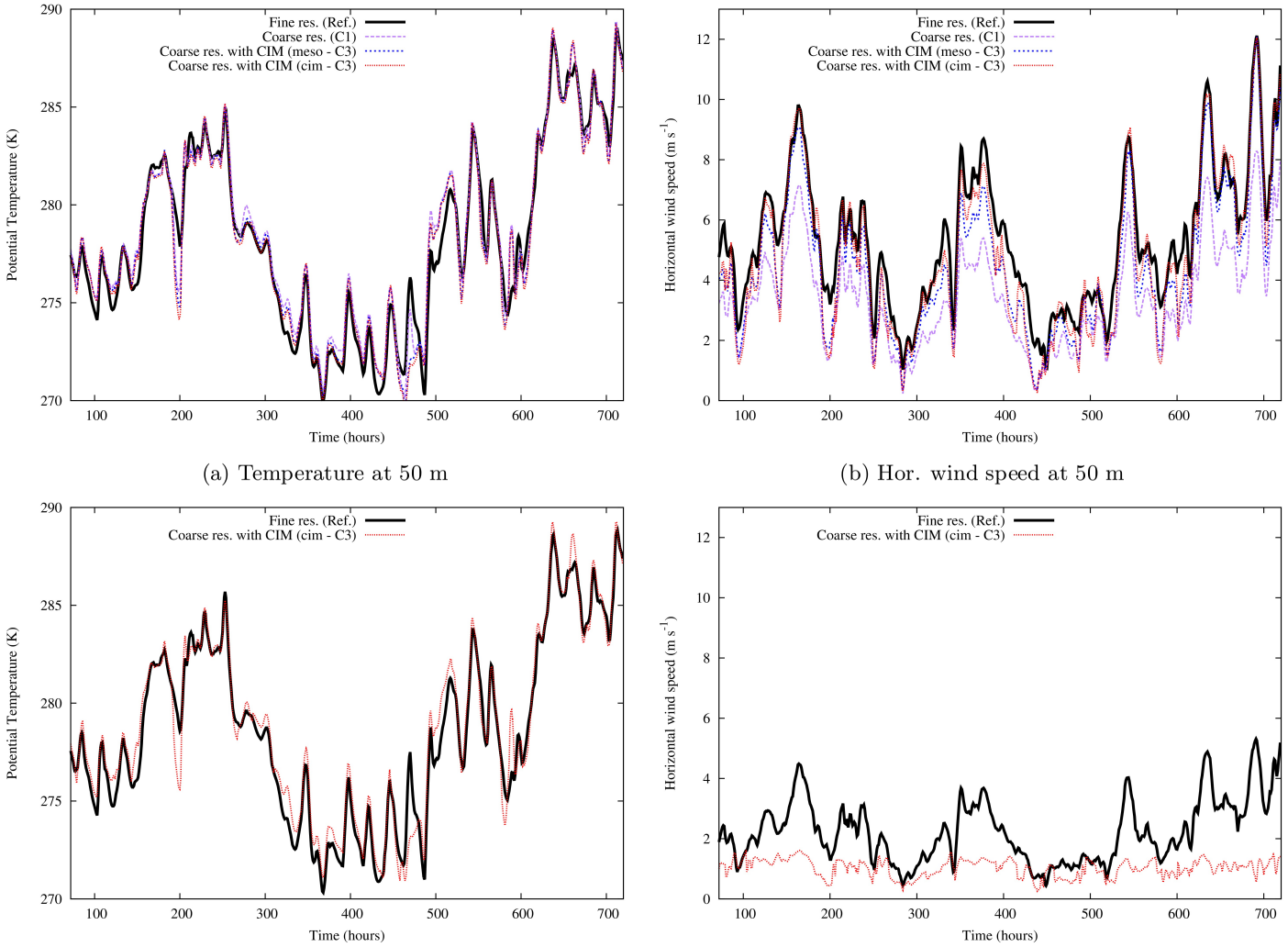

(a) Temperature at 50 m

(b) Hor. wind speed at 50 m

(c) Temperature at 5 m

(d) Hor. wind speed at 5 m

Figure 3: Comparison of the potential temperature (in K) (left) and wind speed (in m s^{-1}) (right) computed using WRF without and with the coupling of the CIM at 50 m (top) and at 5 m (bottom). Black lines refer to reference simulation (Ref.), purple refer to C1, blue lines refer to WRF mesoscale values from C3 (meso - C3) and red lines refer to the CIM values from C3 (cim - C3). Horizontal axis represents the time, in hours, after the start of the simulation

5.1.3. *Effect of the FT coupling - (Ref./C5)*

To show the importance of the coupling methodologies, Table 2 also presents the results of a comparison between the WRF fine resolution simulations and the WRF-CIM simulations without taking into account the horizontal fluxes (C5). It can be noted that when the horizontal fluxes are removed the M.D. and the R.M.S.D. increase for both the temperature and the wind speed as compared to the simulation where the fluxes were present (except for the wind speed at 50 m from the WRF model). The correlation coefficient for the wind speed at 5 m is also drastically reduced.

Even though we know that in the CIM the vertical fluxes and diffusion processes are better taken into account, we cannot conclude that the results are better in this context. The WRF mesoscale model contains a number of processes, such as the horizontal wind advection or pressure gradient, which are not taken into account. It is thus important to take these processes into account in the CIM in such a way that both calculations from the CIM and WRF remain coherent. This thus justifies the use of the FF method.

5.1.4. *Summer results*

Simulations were also performed over a summer period of 1 month in July 2010. Since the results from this period showed similar behaviour to the results for the winter case they will be only briefly discussed here. The integration of the CIM in the WRF model improved the results when comparing to the simulation without the CIM using a coarse resolution. A decrease in the deviation for both the temperature (from 0.5 K to 0.4 K) and the horizontal wind speed (from $-1.1\ \mathrm{m\,s^{-1}}$ to $-0.3\ \mathrm{m\,s^{-1}}$) were noted for the WRF mesoscale data at 50 m. The correlations for the temperature (0.99 to 1) were generally as good as for the winter case. For the profiles calculated by the CIM, it is noteworthy to mention that when the horizontal fluxes were not present, there was a significant increase in difference for the temperature at 5 m (from 0.1 K to 1.8 K) while for the wind speed the results were not remarkably very different for both cases.

5.2. *Comparison on specific vertical profiles*

Selected vertical profiles for specific time steps are chosen to illustrate the effect of the coupling methods in different atmospheric stability conditions. From the time-evolution profiles of the mean wind speed and potential temperature (Fig. 3), we chose some specific periods to plot vertical profiles for one grid cell (the centre of the urban area) for the different scenarios.

5.2.1. *Comparison using a coarse vertical grid resolution in the WRF mesoscale model*

The differences between the profiles calculated by the CIM and by the mesoscale model were studied on an hourly basis and were found to be minimal during the morning when the development of the boundary layer was at a maximum. We thus chose two vertical profiles out of this zone to show that the CIM can perform in near-neutral (stable) or unstable conditions. Figures 4 and 5 show the comparisons of the vertical profiles obtained by the WRF mesoscale model when used at coarse resolution without or with the CIM (Ref., C1 and C3). In the same way as the previous experiences with a high resolution, when the CIM is used, the effect of the FT coupling method is also tested (C5).

At 0200 LT the potential temperature calculate by the WRF mesoscale model (meso-C3) corresponds to the one calculated by the fine resolution WRF simulation (Ref.). At 1700 LT, there is a global difference of less than 0.5 K between the profile calculated (meso-C3) and the fine resolution (Ref.). In both cases the profiles from CIM (cim-C3) are in very good agreement with the Ref. profile. In the absence of horizontal fluxes, the temperature is higher over the whole column of the CIM and the difference is increased to more than 1.5 K in the first 10

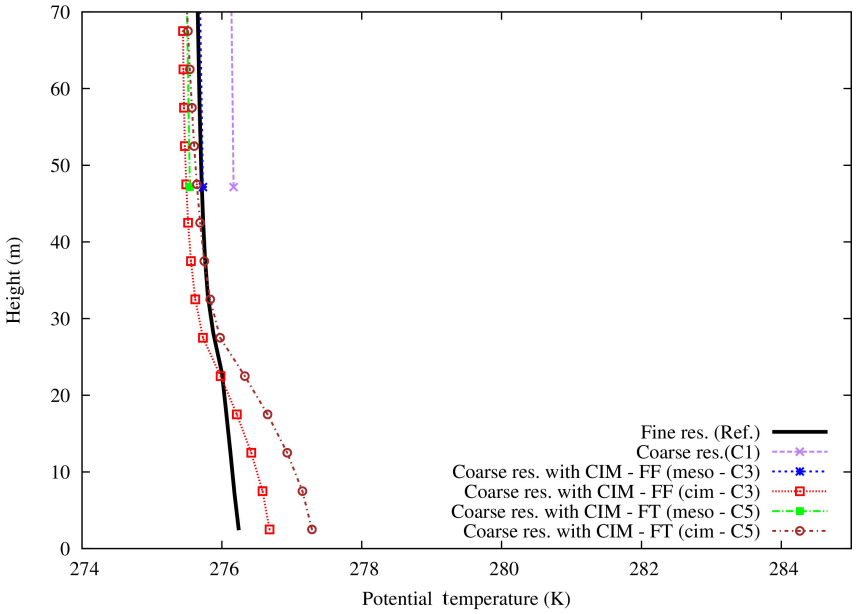

(a) At 0200 LT

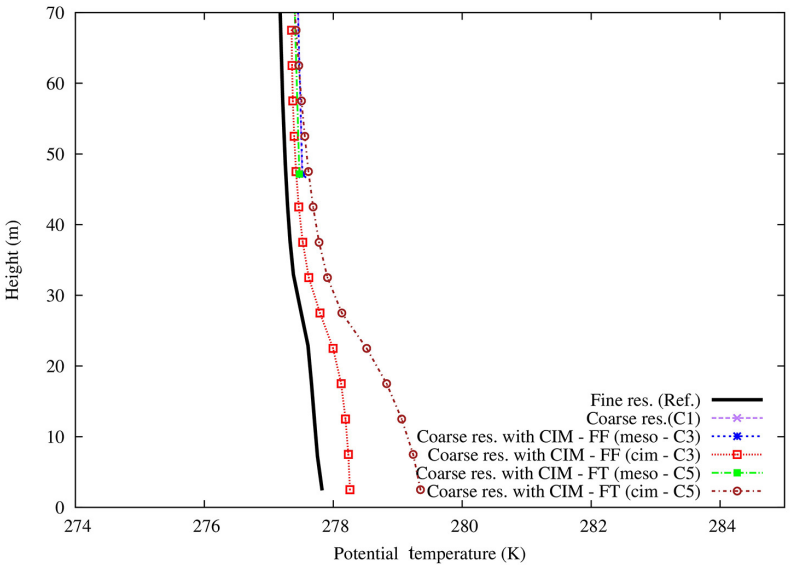

(b) At 1700 LT

Figure 4: Profile of the potential temperature (in K) using a fine resolution with WRF (Ref. - bold black curve), coarse resolution (C1 - purple curve), coarse resolution with the CIM (meso - C3 - blue curve ; cim - C3 - red curve) and coarse resolution with the CIM - with no horizontal fluxes (meso - C5 - green curve ; cim - C5 - brown curve)

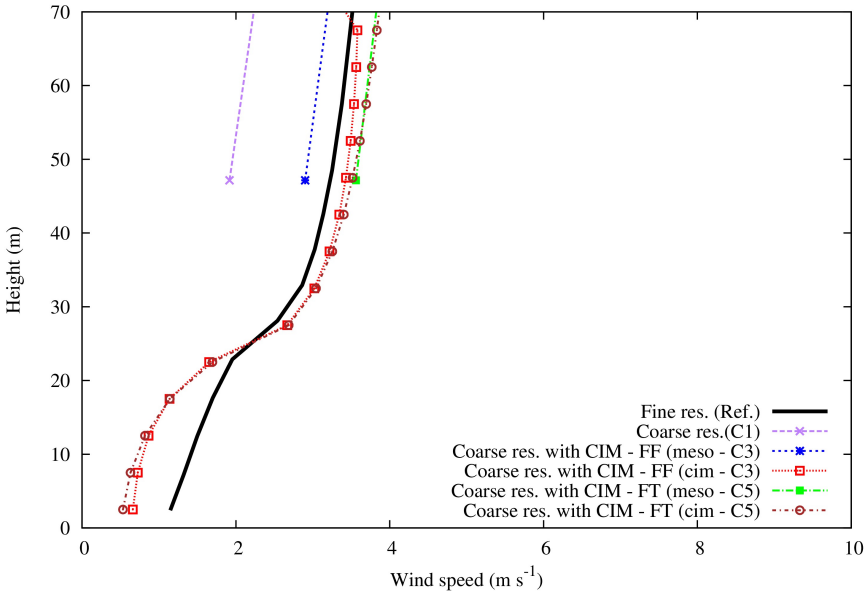

(a) At 0200 LT

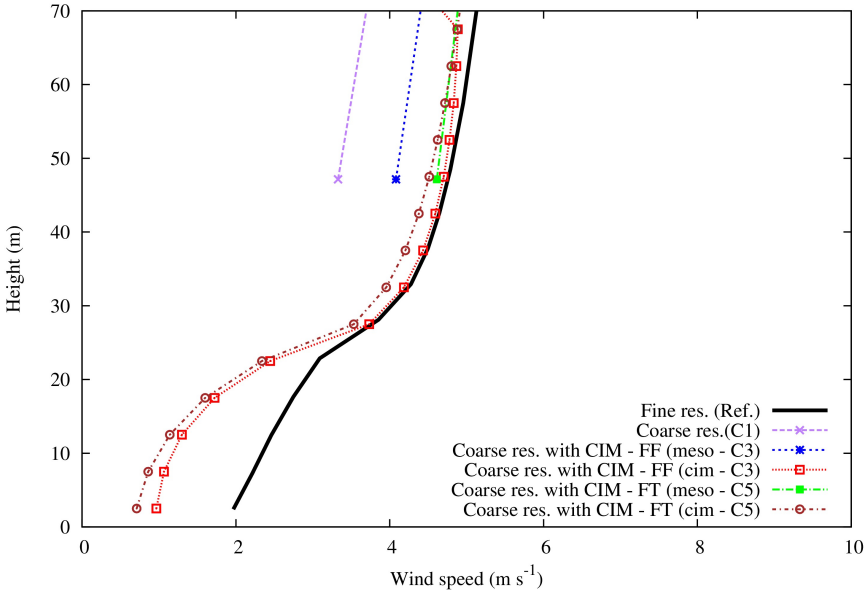

(b) At 1700 LT

Figure 5: Profile of the wind speed (in m s^{-1}) using a fine resolution with WRF (Ref. - bold black curve), coarse resolution (C1 - purple curve), coarse resolution with the CIM (meso - C3 - blue curve ; cim - C3 - red curve) and coarse resolution with the CIM - with no horizontal fluxes (meso - C5 - green curve ; cim - C5 - brown curve)

Table 3: Computational time (in minutes) needed to run the model for 14 days during the winter for each of the simulations.

Simulations	**Computational Time**
Ref.	63 minutes
C1	48 minutes
C3	49 minutes
C5	49 minutes

metres. It is noteworthy to mention that the correction does not change the stability regime of the atmosphere.

In a near-neutral situation, for example at 0200 LT, when using a coarse resolution, the horizontal wind speed of the WRF mesoscale model is closer to the profile Ref. simulation (see Fig. 5a). It can be highlighted here that at 50 m the wind speed rises from 2 $\mathrm{m\,s^{-1}}$ to over 3 $\mathrm{m\,s^{-1}}$. The profiles which are calculated from the CIM are also in very good agreement with the reference simulation. If the horizontal fluxes are removed, the wind speed above the canopy is slightly lower in the CIM.

The results are more contrasted in an unstable condition, such as at 1700 LT (see Fig. 5b). The profile calculated by the CIM, with the horizontal fluxes, is very near to the reference simulation (less than 0.5 $\mathrm{m\,s^{-1}}$ difference). However, if we look at the WRF mesoscale profiles, we can observe that the profile calculated using the method without the horizontal fluxes is much closer to the reference solution. This can also be explained with the method that we have proposed for the calculation of the horizontal fluxes. This correction was defined by using a mean value for the canopy as well as a mean value for the mesoscale model over the corresponding volume. To be in agreement with this statement, if one wants to calculate a coherent profile in the CIM, then there is a slight deterioration of the WRF mesoscale value.

It should also be noted here that in the simulation without horizontal fluxes, the value is fixed at the top boundary conditions. We evaluated in this way two possibilities for fixing the boundary condition at the top. We determined, from these experiments, that the addition of the horizontal fluxes were more important as compared to fixing the top boundary conditions, in order to keep the coherence between both models.

5.3. Computational time

Finally an analysis of the computational time for the simulation performed during the winter time over the 14 days was made. Table 3 summarizes the CPU time used for several simulations.

The data highlights the fact that when the vertical resolution of WRF is decreased, the computational time is significantly decreased (around 25% less). When the CIM is introduced, the computational time is not impacted even though there is an additional calculation which is now being performed by the system to produce high resolution profiles. This means that this coupled WRF-CIM system is able to produce an enhanced simulation without significantly increasing the computational time.

5.4. Validation over Basel using BUBBLE data

The two scenarios described in Sect. 4.2 were run over Basel from the 01/01/2002 to the 14/01/2002. Wind speed and temperature data from the simulation were obtained from a grid cell centred around the coordinates 47.56°N, 7.59°E. This corresponds to the location of the tower installed during the BUBBLE experiment to which the simulated data are compared.

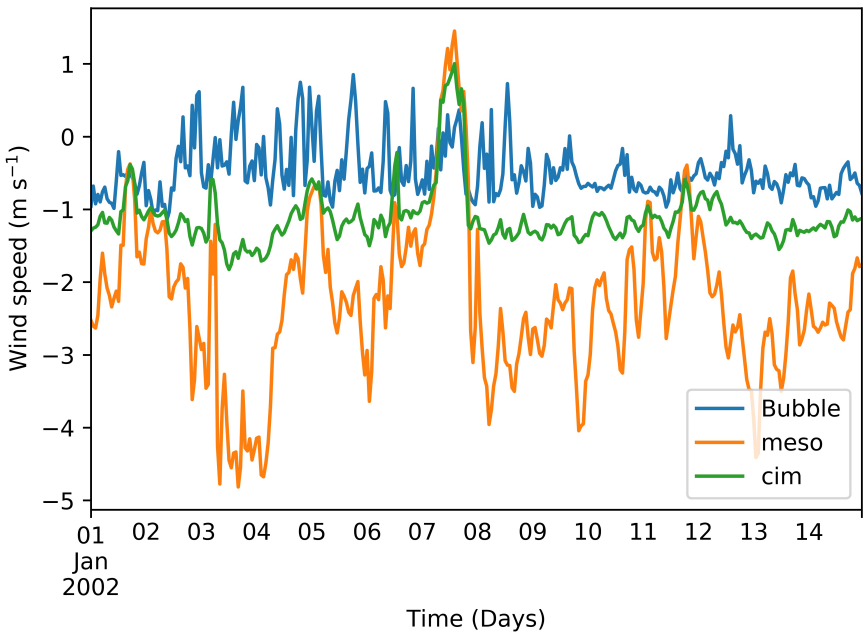

(a) Wind speed in the x-direction

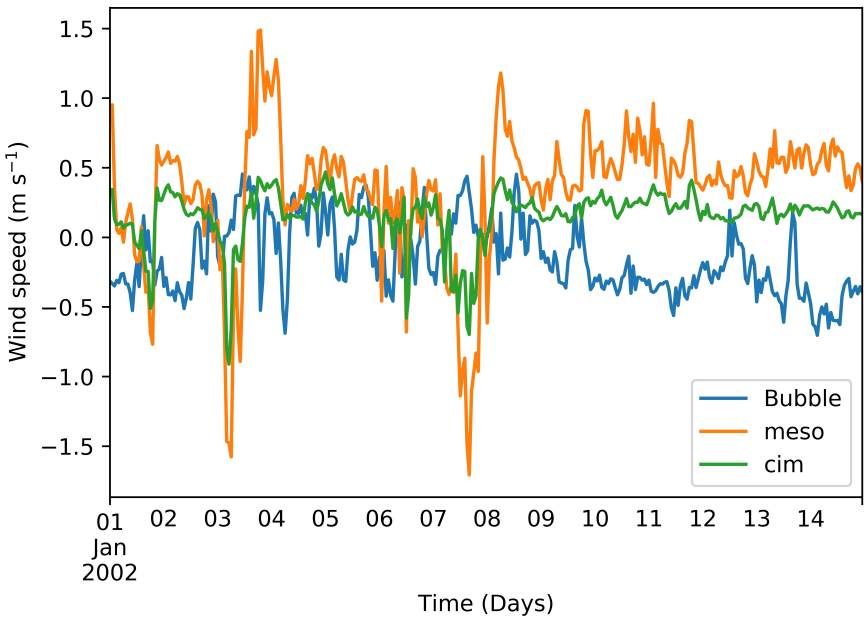

(b) Wind speed in the y-direction

Figure 6: Comparison of the wind speeds (in m s^{-1}) from the BUBBLE experiment (in blue), from WRF mesoscale model(meso - in orange) and from CIM (cim - in green) from the 01/01/2002 to 14/02/2002.

Table 4: Statistical analysis of the simulated data from WRF and CIM against observed data from BUBBLE.

Variable	R.M.S.D	M.D
For Wind ($m\ s^{-1}$)		
BUBBLE-WRF	1.8	-1.5
BUBBLE-CIM	0.5	-0.4
For Potential Temperature (K)		
BUBBLE-WRF	2.6	-0.5
BUBBLE-CIM	2.6	-0.8

Mean deviations represents the deviation from the reference simulation, R.M.S.D is the root mean square error.

Figure 6 shows the wind speed for the x- and y-directions at a height of 3m from the BUBBLE data and from CIM while for the WRF data is the value for the first vertical level typically used for forcing BEP-BEM or any other UCMs in the WRF model. It can clearly be seen that the CIM data is much closer to the BUBBLE data as compared to the WRF data. The difference is more stricking for the u-values. Nonetheless, it is evident that since the WRF data are used as boundary conditions for the CIM, there is a very good correlation between them.

When looking at the horizontal wind speed, the difference is even more visible (see Figure 7a). It can again be highlighted there the CIM data is much closer to the BUBBLE data as compared to the standard WRF data. An statistical analysis of the simulated data and the observational one showed that the R.M.S.D. is reduced from 1.8 $\mathrm{m\,s^{-1}}$ to 0.5 $\mathrm{m\,s^{-1}}$ while the M.D. is notably decreased from -1.5 $\mathrm{m\,s^{-1}}$ to -0.4 $\mathrm{m\,s^{-1}}$ when comparing the BUBBLE data to the WRF and CIM outputs respectively. Figure 7b shows the air temperature as measured by BUBBLE and calculated by WRF and CIM. Both WRF and CIM are able to reproduce the daily dynamics of the air temperature but CIM falls short of improving significantly the results from WRF. This is also reflected in the M.D shown in Table 4 where there is an increase from -0.5 K to -0.8 K. No difference in the R.M.S.D. was noted for the temperature. There are some periods for example on the 12/01 and on the 14/01 where the CIM results are closer to the BUBBLE data but the difference between the simulated and measured data is still around 1 K.. It can be pointed out that the discrepancy between the BUBBLE data and CIM could be due to the over-estimation of the wind speed in some cases, particularly during midday.

6. Discussion and Conclusion

A Canopy Interface Model (CIM) was designed by Mauree et al. (2017a) in such a way that it can act as an interface between mesoscale models and microscale models. In this study it has been coupled with the Weather Research and Forecasting model (WRF). The aim of this study was to evaluate the coupling done specially to improve surface representation in mesoscale models and to demonstrate the ability of the system to provide valuable high-resolution vertical profiles. The CIM is a standalone 1-D column model that can be forced only at the top using values interpolated from the mesoscale model to calculate meteorological profiles independently of the mesoscale model. However to keep the coherence between both the CIM and WRF, a new method, similar to a nudging technique, was determined to add an additional term, in the CIM calculations, to take keep the consistency between the two models.

Using a theoretical setup and a series of sensitivity analysis and simulations, it was shown that:

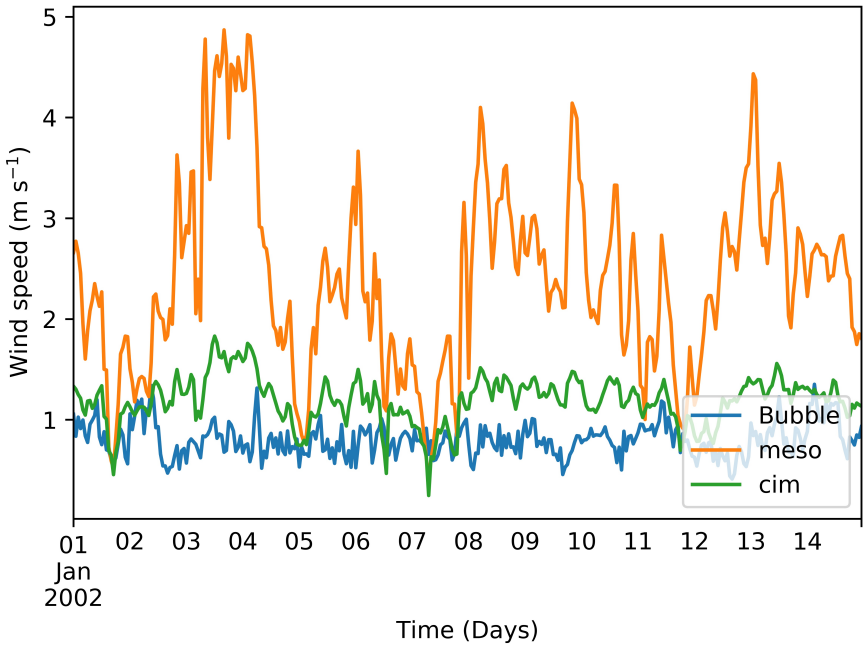

(a) Horizontal wind speed (in m s^{-1})

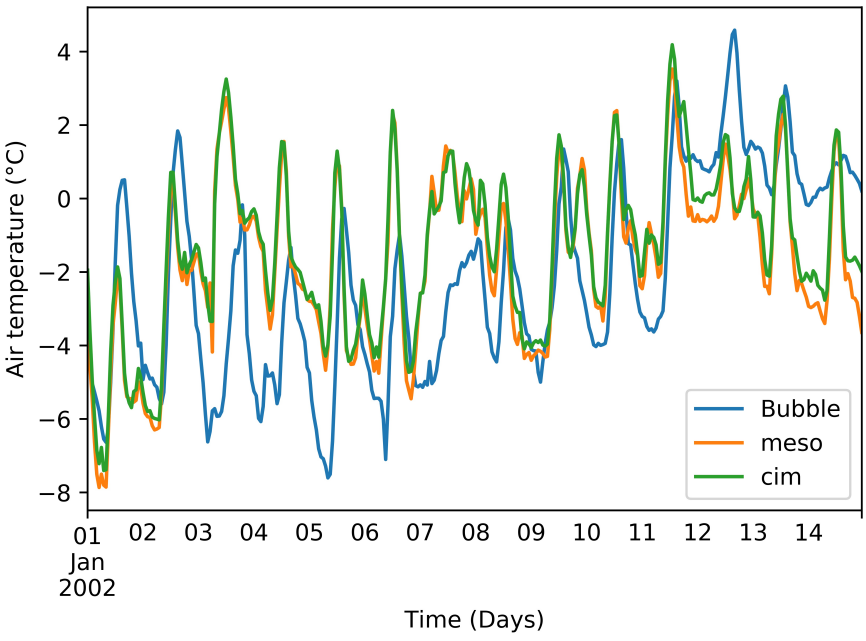

(b) Air temprature (°C)

Figure 7: Comparison of the horizontal wind speed (in m s^{-1}) and the air temperature (°C) from the BUBBLE experiment (in blue), from WRF mesoscale model (meso - in orange) and from CIM (cim - in green) from the 01/01/2002 to 14/02/2002.

- When WRF was used with a coarse resolution, the coupling of the CIM and WRF was closer to the reference simulations. We also verified that when WRF was used with a high vertical resolution similar to the CIM (5 m), the simulated profiles of both models were very similar and in this way coherent. Compared to the highly resolved simulation, it was shown that WRF, with a low resolution, tends to compute higher temperatures and lower the wind speeds. Coupled with the CIM, the new system yielded smaller R.M.S.D and deviations. Usually the correlations were similar and very good.

- It was demonstrated that the correction brought to the CIM calculation to take into account the horizontal fluxes was very important in order for both the WRF mesoscale model and the CIM to be in coherence.

Not all of the experiments that were conducted were presented here. A simulation was carried out for a summer period and as the results showed similar behavior to the results presented in this study, they were only briefly discussed. Tests were also conducted to evaluate the influence of fixing a value at the top of the canopy or calculating a flux. There were no significant changes between the two scenarios, but it is more coherent to use a flux instead of fixing a value at the top based on the method that we have described. This provides an enhanced degree of freedom for the calculation in the CIM. We also analyzed the influence of having different vertical resolutions for the first mesoscale grid cell. This did not show significant impact on the results and therefore means that the CIM can be used independently of the height of the first level in the mesoscale model. The assumption made, when describing the method "FF", that the flux at the top of the canopy has to be equal to the bottom flux, imposes that a constant-flux layer needs to fully develop at the top of the column. It is thus essential to have a minimum number of vertical levels in the CIM to achieve the best performance. It has previously been suggested that the constant-flux layer developed at a height of twice the maximum height of the buildings (Rotach, 1999). This can thus be used as an indication of the number of levels required in CIM.

One important point was also that to demonstrate that if the city is large, CIM could also improve larger scale simulations than urban scale simulations (important information for studies and simulations run at a much larger scale). Some previous studies (Best et al., 2006; Essery et al., 2003; Oleson et al., 2008) have included urban surface schemes in global circulation models using a much coarser horizontal resolution but there is still a need to improve these parameterization and for local-scale feedbacks (Vautard et al., 2013). This is where it is expected that CIM could bridge the gap in these models and hence whatever the scale of grid cell, the use of CIM-BEP-BEM can be discussed and the most appropriate modelling strategy can be chosen.

Furthermore, we validated the high-resolution vertical profiles by comparing the simulated profiles from WRF and from CIM with data from the BUBBLE experiments. We demonstrated that the horizontal wind speed was very close to the observed BUBBLE data and that there were good agreement with the air temperature simulations. There are however some discrepancies in the simulations which can further be investigated in the future. One example is that the wind speed is still slightly over-estimated and this might be due to the parameterization of the drag-force.

Further investigations are required to improve our comprehension of the processes taking place at these different scales. The resolution of the turbulence closure in the CIM is different from that of WRF: this would explain why close to the surface the CIM has a higher impact than far enough from the surface. Moreover when a correction was brought to the CIM in such a way that the CIM calculations were coherent with the WRF mesoscale calculation, this meant that the results in the WRF mesoscale models were less affected in some cases, particularly in unstable conditions. The WRF+CIM+BEP-BEM system also has to be tested on a more realistic domain so that measured monitored data can be compared with the simulation results. An observational

campaign (MoTUS), measuring high resolution and high-frequency variables has been launched on the EPFL campus, Switzerland to develop new parameterizations (Mauree et al., 2017d).

In conclusion of this study, we can say that the WRF+CIM+BEP-BEM system is able to calculate coherent high resolution vertical profiles in the canopy and these profiles were in good agreement with those calculated using WRF with a high vertical grid resolution. It was therefore demonstrated that the CIM can be used in a low-vertical resolution mesoscale model to reduce the computational cost and to improve results. In view of the above promising results, the foundation for the use of the CIM as an interface to enhance surface representation and to couple mesoscale models to microscale models is established.

7. Acknowledgements

The authors would like to thank ADEME, Region Alsace, REALISE, ZAEU for financial supports. This work was partially done in the framework of the SCCER Future Energy Efficient Buildings and Districts, FEEB&D (CTI.2014.0119), the ANR Trame Verte and the CCTV2 projects. The authors thank the High Performance Computing Centre of the Université de Strasbourg (http://hpc.unistra.fr) where the system WRF-CIM was set-up and where the servers were partially funded via the french Equipex project Equip@Meso. We would also like to thank Alberto Martilli for the interesting discussions and Andreas Christen for the BUBBLE data.

8. References

Ashie Y, Thanh Ca V, Asaeda T 1999 Building canopy model for the analysis of urban climate. J Wind Eng Ind Aerodyn 81:237-248. DOI 10.1016/S0167-6105(99)00020-3

Baklanov A, Grimmond CS., Mahura A, Athanassiadou M 2009 Meteorological and air quality models for urban areas. Springer

Best MJ, Grimmond CSB, Villani MG, 2006 Evaluation of the urban tile in MOSES using surface energy balance observations 118 (3), 503–525. DOI 10.1007/s10546-005-9025-5

Bougeault P, Lacarrère P 1989 Parameterization of orography-induced turbulence in a mesobeta-scale model. Mon Weather Rev 117:1872-1890.

Bruse M, Fleer H 1998 Simulating surface-plant-air interactions inside urban environments with a three dimensional numerical model. Environ Modell Softw 13:373-384. DOI 10.1016/S1364-8152(98)00042-5

Chen F, Dudhia J 2001 Coupling an advanced land surface-hydrology model with the Penn State-NCAR MM5 modeling system. Part I: Model implementation and sensitivity. Mon Weather Rev 129:569-585.

Ching JKS 2013 A perspective on urban canopy layer modeling for weather, climate and air quality applications. Urban Climate 3:13-39. DOI 10.1016/j.uclim.2013.02.001.

Crawley DB, Hand JW, Kummert M, Griffith BT 2008 Contrasting the capabilities of building energy performance simulation programs. Build Environ 43:661-673. DOI 10.1016/j.buildenv.2006.10.027

Essery RLH, Best MJ, Betts RA, Cox PM, Taylor CM 2003 Explicit representation of subgrid heterogeneity in a GCM land surface scheme 4 (3), 530–543.

Garuma GF 2017 Review of urban surface parameterizations for numerical climate models. Urban Climate. DOI 10.1016/j.uclim.2017.10.006.

Kanda M, Kawai T, Kanega M, et al 2005 A simple energy balance model for regular building arrays. Boundary-Layer Meteorol 116:423-443. DOI 10.1007/s10546-004-7956-x

Kikegawa Y, Genchi Y, Yoshikado H, Kondo H 2003 Development of a numerical simulation system toward comprehensive assessments of urban warming countermeasures including their impacts upon the urban buildings' energy-demands. Appl Energy 76:449-466. DOI 10.1016/S0306-2619(03)00009-6

Kondo H, Genchi Y, Kikegawa Y, et al 2005 Development of a multi-layer urban canopy model for the analysis of energy consumption in a big city: Structure of the urban canopy model and its basic performance. Boundary-Layer Meteorol 116:395-421. DOI 10.1007/s10546-005-0905-5

Krpo A, Salamanca F, Martilli A, Clappier A 2010 On the impact of anthropogenic heat fluxes on the urban boundary layer: A two-dimensional numerical study. Boundary-Layer Meteorol 136:105-127. DOI 10.1007/s10546-010-9491-2

Kusaka H, Kondo H, Kikegawa Y, Kimura F 2001 A simple single-layer urban canopy model for atmospheric models: comparison with multi-layer and slab models. Boundary-Layer Meteorol 101:329-358. DOI 10.1023/A:1019207923078

Kusaka, H., Kimura, F., 2004. Thermal effects of urban canyon structure on the nocturnal heat island: Numerical experiment using a mesoscale model coupled with an urban canopy model. J Appl Meteorol 43 (12), 1899-1910.

Liu Y, Chen F, Warner T, Basara J 2006 Verification of a mesoscale data-assimilation and forecasting system for the Oklahoma City area during the Joint Urban 2003 field project. J Appl Meteorol Clim 45:912-929.

Martilli A, Clappier A, Rotach MW 2002 An urban surface exchange parameterisation for mesoscale models. Boundary-Layer Meteorol 104:261-304. DOI 10.1023/A:1016099921195

Martilli A 2007 Current research and future challenges in urban mesoscale modelling. Int J Climatol 27:1909-1918. DOI 10.1002/joc.1620

Masson V 2000 A physically-based scheme for the urban energy budget in atmospheric models. Boundary-Layer Meteorol 94:357-397. DOI 10.1023/A:1002463829265

Mauree D 2014 Development of a multi-scale meteorological system to improve urban climate modeling. PhD thesis. Université de Strasbourg

Mauree D, Kaempf J H, Scartezzini J-L, 2015. Multi-scale modelling to improve climate data for building energy models. In: Proceedings of the 14th International Conference of the International Building Performance Simulation Association. Hyderabad.

Mauree D, Blond N, Kohler M, Clappier A 2017 On the coherence in the boundary Layer: Development of a Canopy Interface Model. Front. Earth Sci. 4:109. DOI 10.3389/feart.2016.00109

Mauree D, Coccolo S, Kaempf J, Scartezzini J-L 2017. Multi-scale modelling to evaluate building energy consumption at the neighbourhood scale. PLOS ONE 12 (9): e0183437. DOI 10.1371/journal.pone.0183437.

584 Mauree D, Perera A T D, Scartezzini J-L 2017. Influence of Buildings Configuration on the
585 Energy Demand and Sizing of Energy Systems in an Urban Context. Energy Procedia, 142 :
586 2648-54. DOI 10.1016/j.egypro.2017.12.206.

587 Mauree D, Sang-Hoon Lee D, Naboni E, Coccolo S, Scartezzini J-L 2017. Localized meteorological
588 variables influence at the early design stage. Energy Procedia,122 : 325-30. DOI 10.1016/j.
589 egypro.2017.07.331.

590 Mauree D, Coccolo S, Perera ATD, Nik V, Scartezzini J-L, Naboni E 2018 A new framework to
591 evaluate urban design using urban microclimatic modeling in future climatic conditions 10 (4),
592 1134. DOI 10.3390/su10041134

593 Monin AS, Obukhov AM 1954 Basic laws of turbulent mixing in the surface layer of the atmo-
594 sphere. Contrib Geophys Inst Acad Sci USSR 151:163-187.

595 Muller C 2007 Improvement of an urban turbulence parametrization for meteorological opera-
596 tional forecast and air quality modeling. PhD thesis. École Polytechnique Fédérale de Lausanne

597 National Centers for Environmental Prediction/National Weather Service/NOAA/U.S. Depart-
598 ment of Commerce. Updated daily. NCEP FNL Operational Model Global Tropospheric Anal-
599 yses, continuing from July 1999. Research Data Archive at the National Center for Atmospheric
600 Research, Computational and Information Systems Laboratory. Accessed 15 Sep 2017. DOI
601 10.5065/D6M043C6

602 Oke TR 1982 The energetic basis of the urban heat island. Q J R Meteorol Soc 108:1-24. DOI
603 10.1002/qj.49710845502

604 Oleson KW, Bonan G, Feddema J, Vertenstein M 2008 An urban parameterization for a global
605 climate model. part II: Sensitivity to input parameters and the simulated urban heat island in
606 offline simulations 47 (4), 1061–1076.

607 Omrani H, Drobinski P, Dubos T 2015. Using nudging to improve global-regional dynamic consis-
608 tency in limited-area climate modeling: What should we nudge? Clim Dyn 44 (5-6), 1627–1644.

609 Ooyama KV 1990 A thermodynamic foundation for modeling the moist atmosphere. J Atmos
610 Sci 47:2580-2593.

611 Perera ATD, Coccolo S, Scartezzini J-L, Mauree D, 2018 Quantifying the impact of urban climate
612 by extending the boundaries of urban energy system modeling 222, 847–860.

613 Pohl B, Crétat J, Sep. 2014. On the use of nudging techniques for regional climate mod-
614 eling: application for tropical convection. Clim Dyn 43 (5-6), 1693-1714. DOI 10.1007/
615 s00382-013-1994-3

616 Rotach MW, 1999. On the influence of the urban roughness sublayer on turbulence and disper-
617 sion, Atmos Environ 33 (24): 4001-4008. DOI 10.1016/S1352-2310(99)00141-7

618 Rotach MW, Vogt R, Bernhofer C, Batchvarova E, Christen A, Clappier A, Feddersen B, et al
619 2005 BUBBLE – an Urban Boundary Layer Meteorology Project. Theor Appl Climatol 81
620 (3-4): 231-61. DOI 10.1007/s00704-004-0117-9.

621 Robinson D Nov. 2012 Computer modelling for sustainable urban design: Physical principles,
622 methods and applications. Routledge.

Salamanca F, Krpo A, Martilli A, Clappier A 2010 A new building energy model coupled with an urban canopy parameterization for urban climate simulations—part II. Validation with one dimension off-line simulations. Theor Appl Climatol 99:345-356. DOI 10.1007/s00704-009-0142-9

Salamanca F, Martilli A, Tewari M, Chen F 2011 A study of the urban boundary layer using different urban parameterizations and high-resolution urban canopy parameters with WRF. J Appl Meteorol Clim 50:1107-1128.

Sarkar A, De Ridder K 2011 The urban heat island intensity of paris: A case study based on a simple urban surface parametrization. Boundary-Layer Meteorol 138:511-520. DOI 10.1007/s10546-010-9568-y

Skamarock WC, Klemp JB, Dudhia J, et al 2008 A description of the advanced research WRF version 2. DTIC Document

Skamarock WC, Klemp JB, Dudhia J, et al 2005 A description of the advanced research WRF version 2. DTIC Document

Vautard R, Gobiet A, Jacob D, Belda M, Colette A, Déqué M, Fernández J, et al 2013 The simulation of european heat waves from an ensemble of regional climate models within the EURO-CORDEX project 41 (9), 2555–2575. DOI 10.1007/s00382-013-1714-z

Appendix A. Supplementary Material

Appendix A.1. Additional experiments

Table A.5: Additional experiments run for theoretical case.

Simulations	**Designation**	**Vertical resolution**	**Method**
BEP-BEM+CIM	C2	Fine res. - 5 m (15 levels)	FF
BEP-BEM+CIM	C4	Fine res. - 5 m (15 levels)	FT

FF (fixed flux) and FT (fixed top) represent the two coupling methods.

WRF is run for all the simulations using the BEP-BEM parameterization for the urban effects. The vertical resolution for both WRF and CIM are similar (5 m). The choice of the method are changed for the different scenarios:
Simulation C2 : WRF is run with the vertical resolution of the Ref. simulation and with the CIM coupled using Method FF. The BEP-BEM parametrization runs with the profiles calculated by the CIM. This simulation is carried out to test whether the CIM has a significant effect when WRF is running with a high resolution.
Simulation C4 : WRF is run with the vertical resolution of the Ref. simulation and with the CIM coupled using Method FT. This test is done to compare with the FF method.

Table A.6: Statistical comparison between the Reference Simulation (Ref.) and simulations C2 and C4.

Simulations	**Method**				
	FF	**FT**	**Mean bias**	**R.M.S.E**	**R**
For Potential Temperature (K)					
WRF+CIM+BEP-BEM					
Meso outputs at 50 m					
Fine Res. C2	x		0.0	0.1	1.00
Fine Res. C4		x	−0.1	0.3	1.00
For Wind ($m\ s^{-1}$)					
WRF+CIM+BEP-BEM					
Meso outputs at 50 m					
Fine Res. C2	x		0.2	0.3	1.00
Fine Res. C4		x	0.6	0.8	0.99

All simulations are run for the same winter period described in Sect. 4.1. Comparisons are made for all the mesoscale outputs C2 and C4. FF (fixed flux) and FT (fixed top) represent the two coupling methods. Mean bias represents the deviation from the reference simulation, R.M.S.E is the root mean square error and R is the correlation. Meso outputs refers to outputs from the mesoscale model WRF at 50m which refers to the height at which the data is taken.

Appendix A.1.1. Comparison using a fine vertical grid resolution in the mesoscale model

Appendix A.1.2. Effect of the FF coupling with the CIM at high resolution - (Ref./C2)

As expected the introduction the CIM in WRF with a high vertical resolution in the mesoscale model (C2) did not have a significant impact on the simulation. Indeed, its was shown that the mesoscale simulations were not considerably modified when using a fine vertical grid resolution in WRF. One can note from Table A.6 that the comparison with the high resolution simulation with the CIM gives satisfactory correlations. There were no difference on average for temperature and a small positive mean deviation for the wind speed. It can hence be asserted that the CIM is not bringing noteworthy changes in the WRF simulations when a very fine resolution is used and hence that it is not deteriorating an already enhanced mesoscale simulation.

Figures Appendix A.1 and Appendix A.2 show the comparison between the vertical profiles obtained by the mesoscale model when used at high resolution with or without the CIM (Ref. and C2). We can note that the temperature profiles from the mesoscale model is not modified while the wind speed profile is slightly above the Ref. simulation. When the CIM is used, the effect of the horizontal coupling is also tested by removing the horizontal fluxes in the CIM computation (C4). It turns out that the CIM with the horizontal fluxes gives profiles for the temperature and wind that are closer to the reference simulation, at both times in near-neutral or unstable conditions. However, when these fluxes are not taken into account, there are changes in the profiles both at the mesoscale level and in the CIM. The temperature is higher (e.g., 1 K at 1700 LT in the CIM) near the surface while the wind speed is further considerably lower than in the mesoscale model.

The effect of the FF method can be noted on the profiles at 0200 LT with a disconnection at the top of the column between CIM's profile and the mesoscale profile. This is due to the fact that the correction forces CIM to give a mean value equal to the mesoscale mean value. This is however not observed when the mixing is important (at 1700 LT).

678

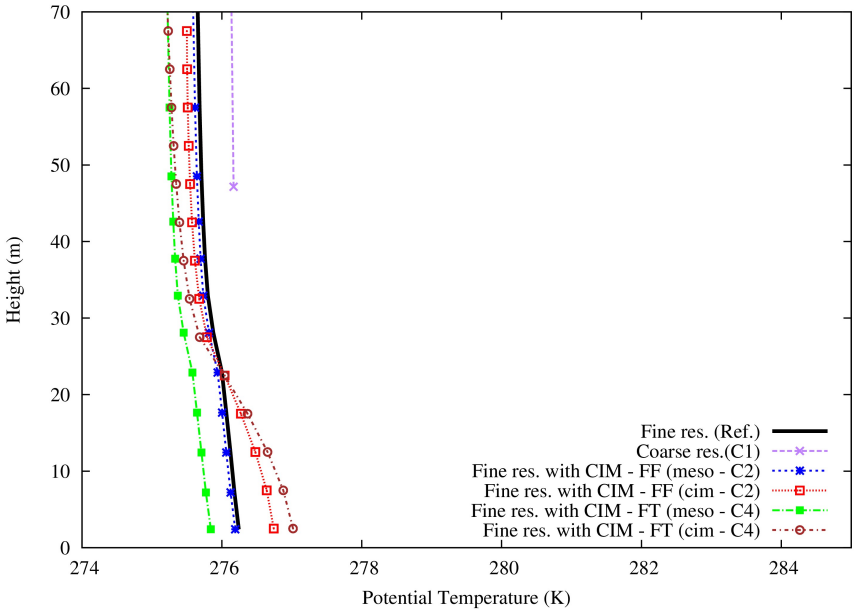

(a) At 0200 LT

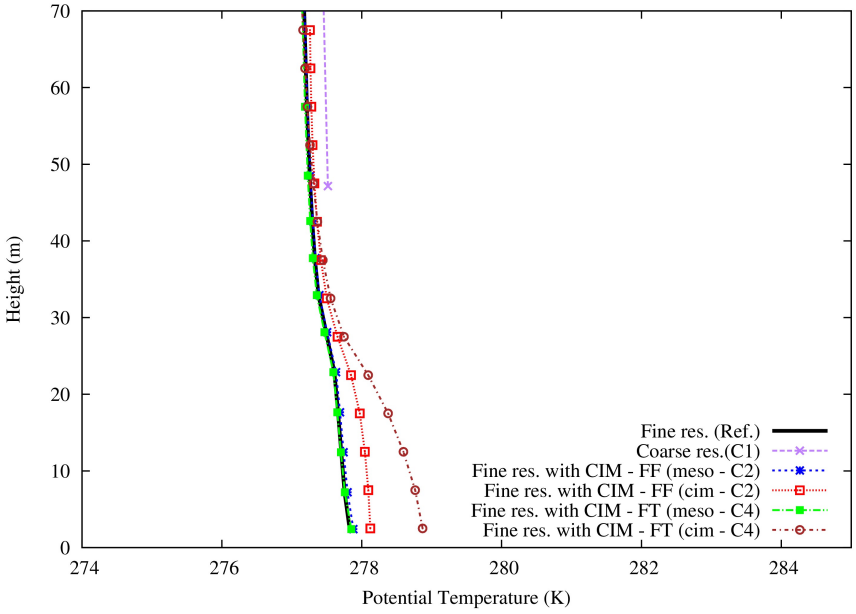

(b) At 1700 LT

Figure Appendix A.1: Profile of the potential temperature (in K) using a fine resolution (Ref. - bold black curve), coarse resolution (C1 - purple curve), fine resolution with the CIM (meso - C2 - blue curve ; cim - C2 - red curve) and fine resolution with the CIM - with no horizontal fluxes (meso - C4 - green curve ; cim - C4 - brown curve)

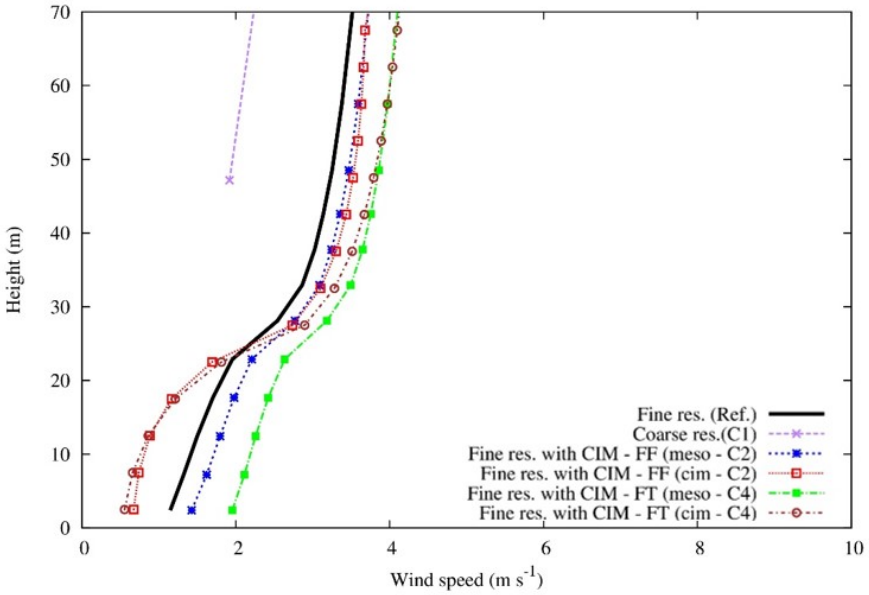

(a) At 0200 LT

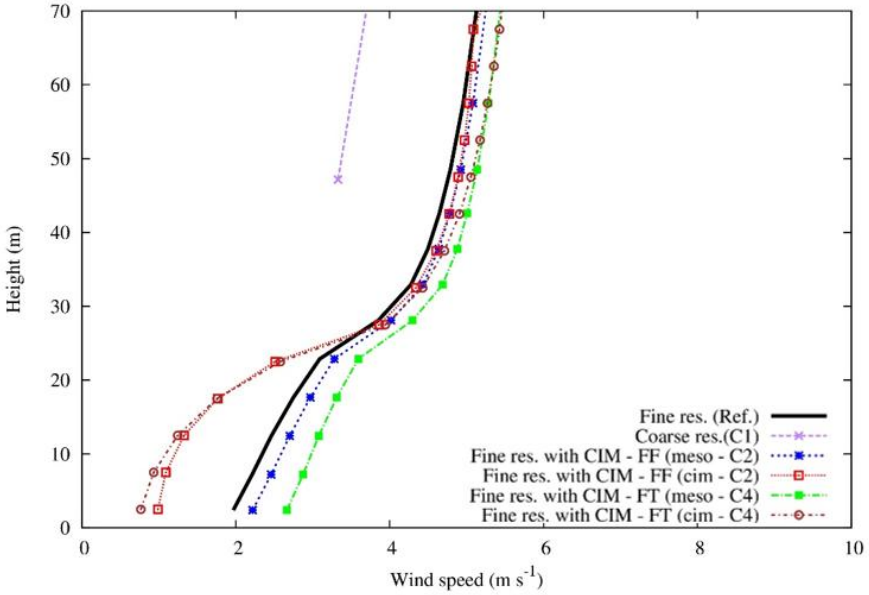

(b) At 1700 LT

Figure Appendix A.2: Profile of the wind speed (in m s^{-1}) using a fine resolution with WRF (Ref. - bold black curve), coarse resolution (C1 - purple curve), fine resolution with the CIM (meso - C2 - blue curve ; cim - C2 - red curve) and fine resolution with the CIM - with no horizontal fluxes (meso - C4 - green curve ; cim - C4 - brown curve)